Microb Ecol (2013) 66:268–280
DOI 10.1007/s00248-013-0180-9

ENVIRONMENTAL MICROBIOLOGY

Contrasting Patterns of Community Assembly in the Stratified Water Column of Great Salt Lake, Utah

Jonathan E. Meuser · Bonnie K. Baxter · John R. Spear · John W. Peters · Matthew C. Posewitz · Eric S. Boyd

Received: 24 October 2012 / Accepted: 9 January 2013 / Published online: 25 January 2013

Abstract Phylogenetic examinations of communities sampled along geochemical gradients provide a framework for inferring the relative importance of niche-based ecological interactions (competition, environmental filtering) and neutral-based evolutionary interactions in structuring biodiversity. Great Salt Lake (GSL) in Utah exhibits strong spatial gradients due to both seasonal variation in freshwater input into the watershed and restricted fluid flow within North America's largest saline terminal lake ecosystem. Here, we examine the phylogenetic structure and composition of archaeal, bacterial, and eukaryal small subunit (SSU) rRNA genes sampled along a stratified water column (DWR3) in the south arm of GSL in order to infer the underlying mechanism of community assembly. Communities sampled from the DWR3 epilimnion were phylogenetically clustered (i.e., coexistence of close relatives due to environmental filtering) whereas those sampled from the DWR3 hypolimnion were phylogenetically overdispersed (i.e., coexistence of distant relatives due to competitive interactions), with minimal evidence for a role for neutral processes in structuring any assemblage. The shift from phylogenetically clustered to overdispersed assemblages was associated with an increase in salinity and a decrease in dissolved O_2 (DO) concentration. Likewise, the phylogenetic diversity and phylogenetic similarity of assemblages was strongly associated with salinity or DO gradients. Thus, salinity and/or DO appeared to influence the mechanism of community assembly as well as the phylogenetic diversity and composition of communities. It is proposed that the observed patterns in the phylogenetic composition and structure of DWR3 assemblages are attributable to the meromictic nature of GSL, which prevents significant mixing between the epilimnion and the hypolimnion. This leads to strong physicochemical gradients at the halocline, which are capable of supporting a greater diversity. However, concomitant shifts in nutrient availability (e.g., DO) at and below the halocline drive competitive interactions leading to hypolimnion assemblages with minimal niche overlap.

Electronic supplementary material The online version of this article (doi:10.1007/s00248-013-0180-9) contains supplementary material, which is available to authorized users.

J. E. Meuser · J. R. Spear
Department of Civil and Environmental Engineering,
Colorado School of Mines, Golden, CO 80401, USA

B. K. Baxter
Department of Biology and the Great Salt Lake Institute,
Westminster College, Salt Lake City, UT 84105, USA

J. W. Peters · E. S. Boyd (✉)
Department of Chemistry and Biochemistry,
Montana State University, 103 Chemistry Research Building,
Bozeman, MT 59717, USA
e-mail: eboyd@montana.edu

M. C. Posewitz
Department of Chemistry and Geochemistry,
Colorado School of Mines, Golden, CO 80401, USA

Introduction

To understand the mechanisms that both underlie and control the composition and structure of communities is a central goal for ecologists [1–3]. Recent studies aimed at understanding such mechanisms have focused on how contemporary and historical biological interactions (i.e., competitive, facilitative interactions) and the physiological and ecological characteristics of a species (i.e., environmental filtering) have shaped the phylogenetic structure of microbial communities [4–8]. The competitive exclusion hypothesis states that competitive interactions between closely related species within overlapping fundamental niches limit their coexistence over the long term [9]. Given that closely related species tend to share similar ecological niches (i.e., niche conservatism [2, 10]), competitive interactions lead to communities that are comprised of more distantly related species than would be expected based on the species richness of an assemblage (i.e., phylogenetic overdispersion) [1]. In contrast, environmental filtering relates to constraints imposed by the environment on the physiology of a species, which often lead to communities that are comprised of more closely related species than would be expected based on the species richness of an assemblage (i.e., phylogenetic clustering) [1]. In addition to the deterministic processes described above, stochastic or neutral mechanisms of community assembly are also important in structuring the composition of microbial assemblages. Hubble [11] defined communities subject to neutral assembly mechanisms as those that are structured entirely by ecological drift, random migration, and random speciation abilities. An important distinction of the neutral theory of community assembly is that a community on a per individual level is identical in their probabilities of giving birth, dying, migrating, and speciating. Thus, neutral theory is often considered to be a null hypothesis to niche theory [12].

Both ecological (competitive interactions, habitat filtering) and evolutionary or neutral mechanisms are likely to influence the phylogenetic structure and composition of microbial communities. The extent that each of these factors shapes phylogenetic structure is likely to reflect differences in the system being examined, the scale of the study, and the taxa pool that is being analyzed [12–15]. The comparative analysis of the phylogenetic structure of microbial communities sampled across geochemical gradients has the potential to provide insight into the relative importance of these processes in community assembly and can be used to identify barriers that limit the relative importance of each of these mechanisms [1, 5, 7]. For example, the composition and structure of *Acidobacteria* lineages sampled across an alpine elevational gradient revealed strong patterns of phylogenetic clustering regardless of elevation [5]. Interestingly, *Acidobacteria* lineages sampled across freshwater lake environments with contrasting geochemistry indicate that the extent of phylogenetic clustering appeared to be related to the pH of the lake being examined [8]. Variable evidence for ecological and neutral mechanisms of assembly were observed for guilds of organisms involved in organic carbon fermentation [4], nitrogen fixation [6], and photosynthesis [16] sampled across spatial geochemical gradients in Yellowstone hydrothermal ecosystems. As an example, photosynthetic assemblages sampled from hydrothermal ecosystems exhibited evidence for both phylogenetic clustering and overdispersion; the extent to which the structure of each assemblage reflected these mechanisms of assembly was correlated with pH [16]. In contrast, strong evidence for both ecological and neutral mechanisms of community assembly were detected in fermentative bacteria [4] and nitrogen fixing organisms [6] along geochemical gradients in Yellowstone; the extent to which each of these mechanisms influenced community structure was correlated with fluid pH and conductivity, respectively [4, 6]. These findings suggest the existence of environmental barriers that influence the extent by which various mechanisms of community assembly structure the composition of communities, which may vary at different taxonomic or trophic ranks.

Great Salt Lake (GSL) is the largest lake in the western United States and the fourth largest terminal lake in the world (52,000 km^2) [17]. GSL is a shallow, meromictic lake that exhibits a maximum and a mean depth of ~9.0 and 4.3 m, respectively. The construction of a rock and gravel railroad causeway in the late 1950s segregated the lake into a north and south arm, and the restricted flow of water between these two “arms” resulted in the development of a salinity gradient [18]. The north arm salinity is typically at saturation [~5 M, 270–300 g/L total dissolved solids (TDS)] [19], whereas the salinity in the south arm surface brine is substantially lower (~ 2.5 M, 140–150 g/L TDS) due to freshwater inputs via three rivers. Breaches and seeps under the causeway spanning GSL allow the greater density north arm brine to flow underneath the less dense south arm brine, resulting in the formation of a distinct halocline of moderately hypersaline brine above an almost saturated deep brine layer over hundreds of square kilometers of the lake. This halocline creates additional physical and chemical gradients, including temperature and pH gradients [20, 21], which are likely to influence the function of microbial communities. For example, community productivity associated with microbial communities collected from two sites in the south arm of GSL was shown to vary considerably with water column depth and over an annual cycle, with lower overall productivity during the summer months and in the hypolimnion, both of which were attributed to seasonal variation in influent resource abundance and availability [21].

Here, we examine the phylogenetic structure of archaeal, bacterial, and eukaryal small subunit (SSU) rRNA genes in the water column at one of the Utah Division of Wildlife Resources (DWR) regular GSL monitoring sites, the DWR3 site in the south arm of GSL, in an effort to understand the relative importance of competitive and ecological interactions that shape the assembly of microbial communities. However, because assemblages with similar phylogenetic community structure may differ in their species composition [22], we also quantified changes in the taxonomic (alpha diversity) and phylogenetic composition and diversity (beta diversity) along the vertical transect. The vertical depth profile at DWR3 exhibited significant gradients in salinity, dissolved O_2 (DO), photosynthetically active radiation (PAR), temperature and pH for use in assessing their role and influence on the mechanisms of community assembly and community composition.

Materials and Methods

Site Description and Sample Collection

Samples were collected from one GSL north arm site (NA, latitude 41.437891 longitude −112.668843) and one GSL south arm site (DWR3, latitude 41.16746, longitude −112.6696117) (Fig. 1). For the NA sample, brine was collected by wading out to a depth of 0.5 m and sampling surface water in June, 2006. For the DWR3 samples, brine was collected from a DWR research vessel, first in June, 2006 (0 and 8 m depths) for our initial survey and again in June, 2007 (0, 4, 6, 6.5, and 8 m depths) for the follow-up analyses. Here, a 2-L Kemmerer collection bottle (Wildlife Supply, Yulee, FL, USA) was lowered to each depth sampled, with deionized water rinses between each sampling. Samples were transferred to sterile collection bottles leaving minimal headspace volume, stored on ice and transported to the laboratory. Cells were then pelleted by centrifugation (4,000×g for 15 min at 3 °C) using a Sorvall centrifuge (Thermo Fisher, Waltham, MA,

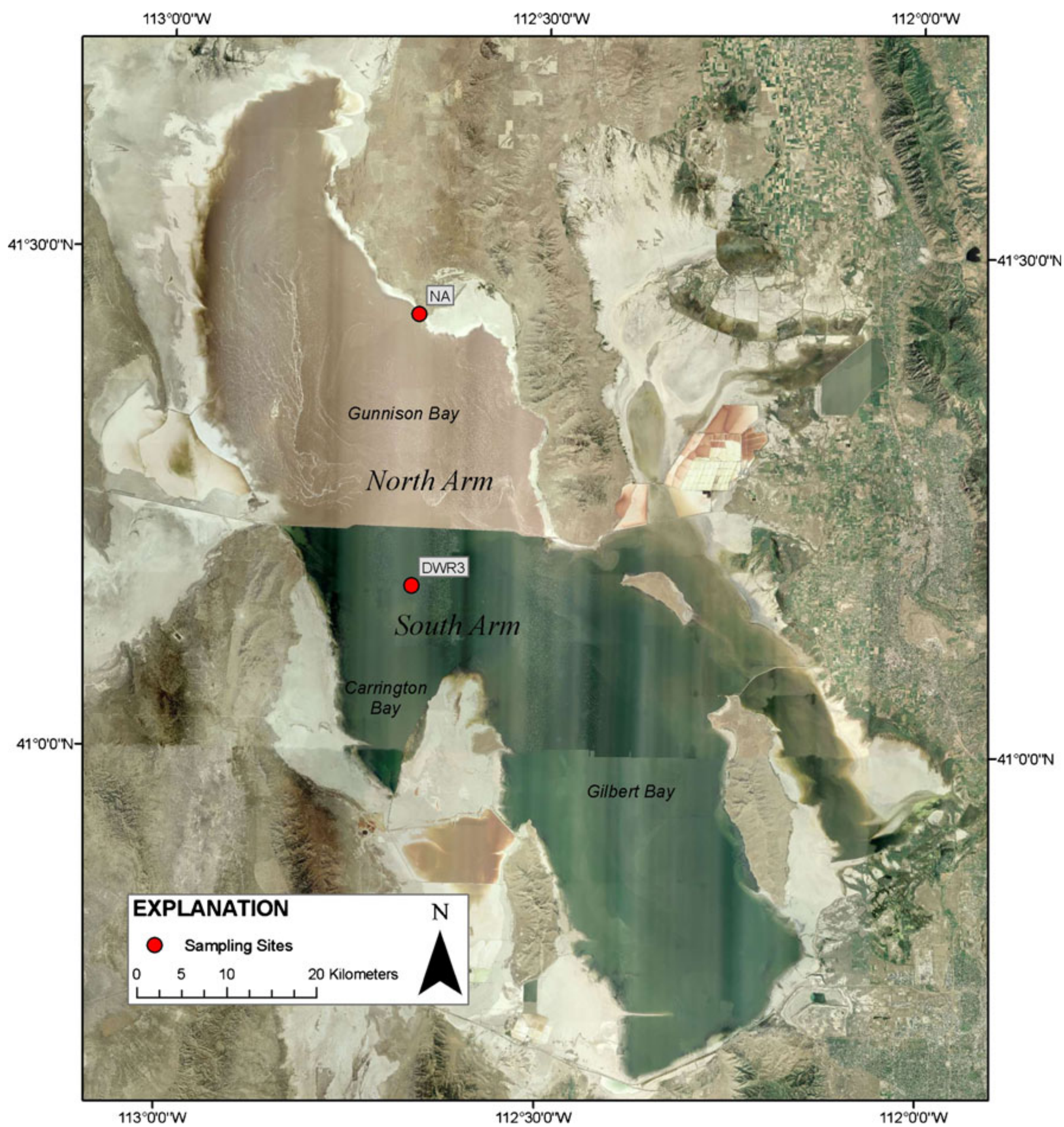

Fig. 1 Satellite image of the GSL with sampling sites where further molecular and geochemical analyses were performed are indicated. The color distinction separating the north arm from the south arm reflects dominance by halophilic archaea and algae, respectively, in the microbial communities of these two basins

USA), the supernatant decanted, and biomass pellets resuspended in 1 mL of supernatant and stored at −80 °C until DNA extraction.

Physical and Chemical Analysis

Environmental parameters were measured concomitant to environmental sampling. Quantum scalar irradiance of total available PAR (μmol 400–700 nm photons $m^{-2}s^{-1}$) was determined using a Li-Cor LI-193 underwater spherical quantum sensor and LI-250A light meter (Li-Cor Biosciences, Lincoln, Nebraska, USA). A Troll 9500 multi-sensor (In-Situ Inc., Fort Collins, CO, USA) was used to simultaneously acquire salinity, DO, temperature and pH at each DWR3 site sampling depth. Filtered GSL DWR3 brine samples were subjected to refractometry to determine salinity. To accurately determine DO response at each depth, 0.2 μM filtered, air-saturated brine samples from each DWR3 depth and the appropriate O_2 solubility equations [23] for NaCl brine were used for probe calibration. pH and temperature values for the 6.5-m depth were interpolated using the variation in salinity observed at this depth, relative to the 6.0 and 8.0 m depth.

DNA Extraction, Cloning, and Sequencing

Total DNA was extracted from resuspended "pea-sized" (approximately 200 mg) pellets of frozen biomass using the PowerSoil™ DNA Isolation Kit (MoBio Inc., Carlsbad, CA, USA) following the manufacturer's instructions with 2 min of bead beating (Mini Beadbeater-8, Biospec Products, Bartlesville, OK, USA) to assist lysis. An initial survey of the NA and DWR3 sites was conducted using universal small subunit (SSU) ribosomal RNA (rRNA) primers. The amplification of SSU rRNA genes from the NA and DWR3 DNA samples were performed using 1 mM concentrations of the forward primer 515 F (5′-GTGCCAGCMGCCGCGGTAA-3′) and reverse primer 1492R (5′-GGTTACCTTGTTACG ACTT-3′) [24]. PCR thermal cycling conditions were as follows: initial denaturation at 94 °C for 2 min, followed by 30 cycles of denaturation (94 °C for 1 min), annealing (55 °C for 1 min) and elongation (72 °C for 1 min). For the DWR3 sample, domain-specific sequence analyses were performed. SSU rRNA gene sequences (16S rRNA for bacteria and archaea; 18S rRNA for eukaryotes) from each environmental sample were amplified using the domain-specific forward primers for bacteria (8F—5′-AGAGTTTGATCCTGGC TCAG-3′), archaea (4F—5′-TCCGGTTGATCCTGCCRG-3′), and eukarya (360FE—5′-CGGAGARGGMGCMT GAGA-3′) in conjunction with the universal reverse primer, 1492R (5′-CCGTCAATTCMTTTRAGTTT-3′) using 1 μL aliquots of total DNA extractions as templates in 25 μL PCR Master Mix reactions (Promega, Madison, WI, USA) with previously described amplification protocols [25]. The resulting amplicons were Montage gel purified (Millipore, Billiceric, MA, USA), and TOPO TA (Invitrogen, Carlsbad, CA) cloned into electrocompetent *E. coli* cells. Three domain-specific libraries of 96 SSU rRNA gene clones were analyzed from each depth sampled at DWR3. Cloned SSU rRNA gene amplicons were sequenced using an ABI 3700 sequencer using the 515F (5′-GACGGCGGTGWGTRCAA-3′) primer. All sequences obtained in this study have been deposited in the GenBank, DDBJ, and EMBL databases under accession numbers JQ952783–JQ953087 (*Archaea*), JQ953088–JQ953419 (*Bacteria*), and JQ953420–JQ953640 (*Eukarya*) (see Supplemental Online Materials).

Sequence Analysis

ClustalX (ver. 2.0.9) [26] was used to align nucleic acid sequences using the International Union of Biochemistry substitution matrix and default gap extension and opening penalties. Since the length of individual reads varied and could bias downstream phylogenetic and community ecological analyses, alignment blocks were first trimmed to an empirically defined length met by ~70 % of the sequences or discarded if defined length requirements were not met. This approach led to a bacterial SSU rRNA gene alignment block containing 332 reads with a uniform length of 416 positions. Likewise, the archaeal SSU rRNA gene alignment block contained 307 reads with a uniform length of 212 positions. The eukaryote SSU rRNA gene alignment block contained 223 reads with a uniform length of 460 aligned positions. There was no observable pattern in the discarded sequences from the bacterial, archaeal, and eukaryote SSU rRNA gene libraries (data not shown). Sequences were checked for chimeric artifacts using Mallard (ver. 1.02) [27] and anomalous sequences were verified using Pintail (ver. 1.0) [28] and these were discarded without further consideration. DOTUR [29] was used to define operational taxonomic units (OTUs) at a sequence identity threshold of 97 % and a precision of 0.01. Rarefaction curves, generated with a sequence identity threshold of 97 %, were used to calculate Chao1 predicted phylotype richness and Simpsons index (D). The reciprocal of the Simpson index ($1/D$) enables direct comparison of assemblage diversity between communities [30], with higher values corresponding to a comparatively greater alpha diversity.

Phylogenetic Analysis

The phylogenetic position of all archaeal, bacterial, and eukaryal SSU rRNA genes was evaluated by approximate likelihood-ratio tests [31] as implemented in PhyML (version 3.0) [32]. Bacterial 16S rRNA gene phylogenies were rooted with SSU rRNA genes from *Acidilobus sulfurireducens* str. 18D70 (EF057391) and *Caldisphaera draconis* str. 18U65

(EF057392). Archaeal 16S rRNA gene phylogenies were rooted with SSU rRNA genes from *Clostridium acetobutylicum* ATCC 824 (AE001437), and *Caldicellulosiruptor saccharolyticus* DSM 8903 (CP000679). Eukaryote SSU rRNA gene phylogenies were rooted with SSU rRNA genes from the protist *Cryptosporidium hominis* isolate W18958 (GQ983354) and the ascomycete *Zygosaccharomyces rouxii* str. CBS732 (CU928181). Phylogenies were constructed using the General Time Reversible substitution model with a proportion of invariable sites and gamma-distributed rate variation as recommended by Modeltest (ver. 3.8) [33]. Phylograms were rate-smoothed using the multidimensional version of Rambaut's parameterization as implemented in PAUP (ver. 4.0) [34]. Rate-smoothing for each phylogram was performed according to the parameters identified using Modeltest. This included the identification of the substitution model, the gamma distribution of rate variation across sites, the proportion of invariant sites, nucleobase frequencies, and the rate matrix for each phylogram.

Community Ecological Analysis

Rate-smoothed cladograms were used to calculate Rao's quadratic entropy (D_P) and the net relatedness index (NRI) specifying among individual abundances (− a parameter) and 999 iterations with the program Phylocom (ver. 4.0.1) [35]. D_P is an abundance-weighted metric that describes the pairwise phylogenetic distance between sequences in a community, when compared to the total sequence pool. Assemblages with higher D_P indices exhibit a greater phylogenetic diversity relative to the total sequence pool. We tested whether NRI values significantly differed from that of a randomly assembled community (null model). Given that the conclusions of the predominant mechanisms influencing the assembly of a community drawn from NRI values can be biased based on the choice of null model for comparison [12], we report the results of NRI indices calculated using all four methods of null model testing available within Phylocom (Supp. Table 1). These include a null model produced by shuffling the phylogeny (null model 0), randomizing the draw of species in the sample pool (null model 1), randomizing the draw of species in the phylogeny pool (null model 2), and the independent swap method (null model 3). Readers are referred to the Phylocom manual for additional details on null models. One thousand permutations were performed and a two-tailed significance test was used to evaluate the rank of observed values. When >900 permutations supported the observed values rather than the random or null model ($p<0.10$), the observed rank was deemed to be significant.

Phylocom was also used to construct Rao among community phylogenetic distance matrices for each cladogram as previously described [36]. Euclidean distance matrices derived from the six environmental variables (i.e., depth, salinity, DO, PAR, temperature, and pH) were constructed using the base package within R (version 2.10.1). With Rao phylogenetic distance as the response variable, model selection through Akaike Information Criteria adjusted for small sample size (AICc) and Mantel regressions were performed to examine relationships with matrices describing individual environmental parameters using the R packages pgirmess (version 1.4.3) (http://pagesperso-orange.fr/giraudoux/) and Ecodist [37], respectively. We considered the model with the lowest AICc value to be the best and evaluated the relative plausibility of each model by examining differences between the AICc value for the best model and values for every other model (ΔAICc) [38].

Results

Screening of Great Salt Lake Biodiversity

An initial probe of microbial community biodiversity was performed at one north arm (NA, 0.5 m depth) and one south arm site (DWR3, surface and 8 m depths) (Fig. 1) to identify an environment with high phylogenetic diversity. Site selection was based on the premise that communities with higher phylogenetic diversity and/or better evidence for phylogenetic structure (assessed using "universal" SSU rRNA gene primers) would provide a better opportunity to identify the variation in phylogenetic composition and structure along the vertical depth gradient. The NA and DWR3 assemblages exhibited statistically significant and positive NRI (5.79 and 5.64, $p<0.01$ and $p<0.01$, respectively, using null model 0) values, suggesting that the surface communities at each site are phylogenetically clustered. Such phylogenetic clustering is indicative of ecological filtering by their local environment whereby closely related species share phenotypic traits that allow them to persist in a given habitat, but not adjacent habitats [7]. An examination of D_P revealed a lower metric for the assemblage sampled from 0.5 m at NA (0.273), than assemblages sampled from the DWR3 surface (0.283) or deep brine (0.356) suggesting that the community inhabiting the DWR3 harbors a greater phylogenetic diversity. Thus, of the two sites, DWR3 was determined to have the best potential to uncover relationships between both the gradients in physicochemistry and the phylogenetic structure and composition of individual archaeal, bacterial, and eukaryal SSU rRNA gene assemblages.

DWR3 Water Column Physicochemistry

Mid-day sampling of the DWR3 water column to a final depth of ~ 8 m revealed gradients in salinity (143 to 247 ppt), DO (0.98 to 5.45 $mg L^{-1}$), PAR (0–1800 $\mu mol m^{-2} s^{-1}$), temperature (16.59 to 24.17 °C), and pH (5.95 to 8.07) (Fig. 2). PAR

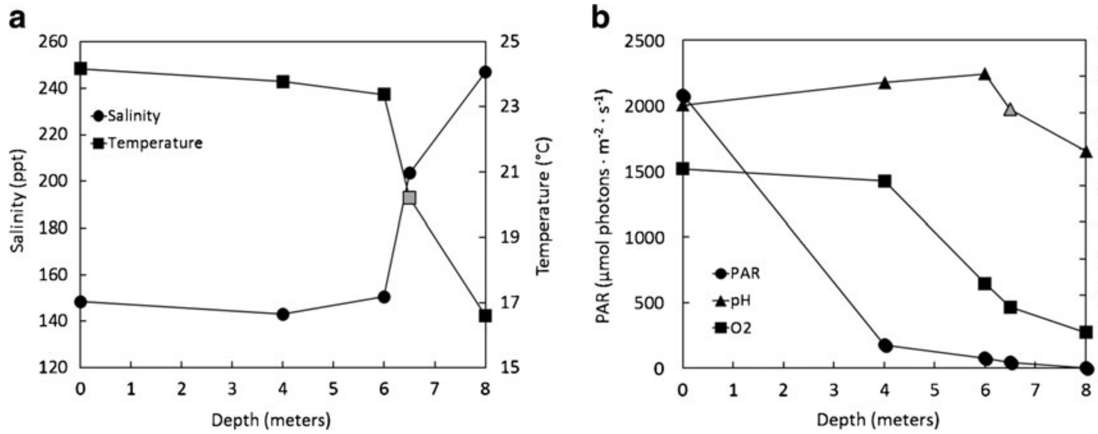

Fig. 2 **a** Salinity and temperature as a function of water column depth. **b** PAR, pH, and DO as a function of water column depth. *Gray points* indicate data that were interpolated

decreased immediately within the first few meters of the DWR3 transect with near total attenuation at a depth of 8 m. A dramatic increase in salinity and decrease in temperature occurred at the deep brine layer at depths of 6.5 to 8 m (Fig. 2a). Additionally, dissolved O_2 levels decreased dramatically at the oxic/anoxic interface (~6 and 6.5 m). The pH increased slightly at 6 m, but was lowest at 8 m. A number of physicochemical parameters co-varied. For example, water column salinity varied inversely with water column temperature (Pearson $R=-0.89$, $p=0.04$) and DO (Pearson $R=-0.99$, $p<0.01$) (data not shown). Water column temperature varied with the pH of the water (Pearson $R=0.87$, $p=0.05$) whereas the DO concentration in the water column varied positively with temperature (Pearson $R=0.83$, $p=0.08$) and inversely with salinity (Pearson $R=-0.81$, $p=0.10$).

Archaeal, Bacterial, and Eukaryal SSU rDNA Sequencing at DWR3

The phylogenetic diversity and structure of archaeal, bacterial, and eukaryal assemblages were characterized along the co-varying physicochemical gradients that make up the DWR3 water column. A total of 307 archaeal, 332 bacterial, and 223 eukaryal SSU rRNA gene sequences that met our length criteria (see "Materials and Methods") were obtained from 5 depths (Table 1). The average depth of sequence coverage was 73.4 % for archaeal assemblages, 49.5 % for bacterial assemblages, and 90.7 % for eukaryal assemblages.

Assessing the Phylogenetic Structure of DWR3 Assemblages

The NRI metric describes the extent by which sequences that comprise an assemblage are clustered on an ultrameric phylogenetic tree. Positive NRI values indicate phylogenetic clustering and suggest that the community is shaped largely by physiological or ecological constraints imposed by the environment (i.e., environmental filtering) whereas negative values indicate phylogenetic overdispersion and suggest that the community is shaped largely by competitive interactions [1]. NRI values that are not statistically significant imply weak competition or environmental filtering and may be suggestive of an important role for neutral processes in community assembly [12]. We first compared the results of NRI values obtained using the four null models available in Phylocom (for a complete description of Phylocom null models, see [35]). All of the NRI metrics revealed similar trends (Supp. Table 1), as indicated by positive and significant correlations when they were regressed against each other (Pearson $R>0.75$ for all comparisons) (data not shown). In particular, NRI metrics determined for archaeal, bacterial, and eukaryal assemblages sampled from the epilimnion using each of the four null models were positive and generally statistically significant (Supp. Table 1), indicating that these assemblages are clustered phylogenetically. Regardless of the null model that is considered, the NRI decreased systematically with depth along DWR3. NRI calculated for archaeal, bacterial, and eukaryal assemblages using null models 0, 1, and 2 were negative in the hypolimnion, although not all were statistically significant (Supp. Table 1, Fig. 3). In contrast, NRI calculated for archaeal, bacterial, and eukaryal assemblages using null model 3 were positive, but not always statistically significant. The discrepancy in the NRI metrics and their statistical significance when calculated using the various null models is likely due to the sensitivity of the models to niche-based mechanisms of assembly versus neutral-based mechanisms of assembly. A previous metacommunity simulation conducted with these four null models found that null models 0, 1, and 2 tend to be more conservative toward identifying patterns in phylogenetic structure that could differentiate niche-based mechanisms of assembly (e.g., environmental filtering or competition) when multiple traits are likely involved in niche assembly in heterogeneous environments [12]. However, care must be exercised in that these same null

Table 1 Clone library statistics for archaeal and bacterial 16S rRNA genes and eukaryl 18S rRNA gene assemblages sampled from each of five depths as determined using DOTUR and a percent identity threshold of 97 %

Archaea					*Bacteria*				*Eukarya*			
Depth (m)	*n*[a]	Chao1[b]	Unique[c]	1/*D*[b]	*n*[a]	Chao1[b]	Unique[c]	1/*D*[b]	*n*[a]	Chao1[b]	Unique[c]	1/*D*[b]
0.0	62	7	6 (85.7)	2.68	66	43	21 (48.8)	6.60	28	2	2 (100.0)	1.08
4.0	13	2	2 (100.0)	2.05	39	22	13 (58.2)	4.01	44	2	2 (100.0)	1.38
6.0	75	36	18 (49.5)	3.61	34	58	26 (45.1)	51.00	68	3	3 (100.0)	1.69
6.5	75	91	36 (39.5)	25.00	82	94	40 (42.5)	27.22	28	6	5 (90.9)	2.39
8.0	82	27	25 (92.3)	17.03	111	109	58 (53.1)	27.75	53	8	5 (62.5)	1.43

[a] Number of clones sequenced

[b] Predicted Chao1 richness and Simpson (D) indices for an assemblage comprising n sequences as determined by DOTUR at a sequence identity threshold of 97 %. The Simpson index D was converted to a diversity index by taking the reciprocal of D ($1/D$)

[c] Number of unique phylotypes sampled from a clone library comprising n sequences as determined by DOTUR at a sequence identity threshold of 97 %, with the coverage of the predicted Chao1 richness indicated in *parentheses*

models are subject to type I errors (false positives) and can detect non-random patterns of phylogenetic structure in communities that are assembled according to neutral mechanisms [12]. Thus, the most conservative interpretation for these observations is that both niche-based competitive interactions and stochastic evolutionary processes are influencing the composition of hypolimnion assemblages.

NRI values observed for each assemblage decrease substantially and sometimes significantly at or below the halocline, where strong gradients in geochemistry are also observed (Fig. 2). Of the environmental parameters measured, NRI values for archaeal, bacterial, and eukaryal assemblages varied most strongly with DO and salinity in the same manner,

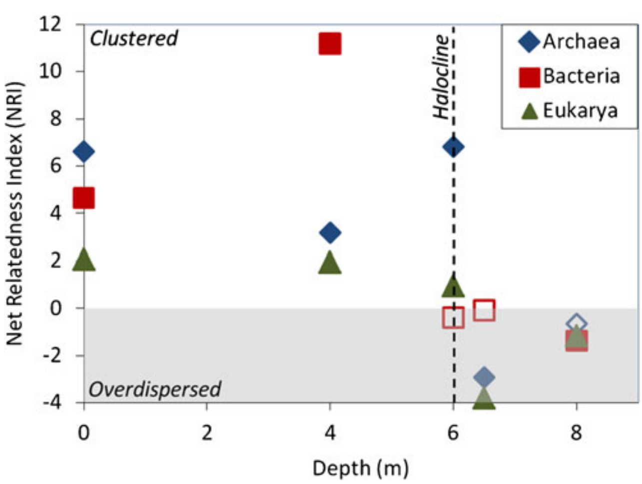

Fig. 3 Variation in archaeal (*blue*), bacterial (*red*), and eukaryal (*green*) phylogenetic relatedness as assessed using the NRI along the DWR3 depth gradient as assessed using null model 0 (see "Materials and Methods"). The *gray box* separates positive NRI values, which indicate phylogenetic clustering, and *negative values*, which indicate phylogenetic overdispersion. Observed community phylogenetic structures unlikely to arise by chance ($p<0.10$) are depicted by *solid symbols*. The halocline, as inferred by salinity measurements at DWR3, is indicated by a *hashed line*

regardless of the null model used to calculate NRI. For example, NRI associated with archaeal, bacterial, and eukaryal SSU rDNA assemblages calculated with null model 0 (Fig. 3) were inversely correlated with salinity (Pearson $R=-0.79$, -0.65, and -0.73, respectively; p values=0.11, 0.23, and 0.16) and positively correlated with DO (Pearson $R=0.62$, 0.86, and 0.78, respectively; p values=0.26, 0.06, and 0.12) (data not shown).

Assessing the Alpha and Beta Diversity of Assemblages

The predicted Chao1 phylotype richness and Simpson diversity indices for archaeal, bacterial, and eukaryal assemblages sampled from each depth generally followed the same trends and tend to co-vary (Fig. 4). The lowest predicted archaeal, bacterial, and eukaryal Simpson diversity was observed from the surface to a depth of 4 m. At depths ranging from 4 to 6 m, the Simpson diversity indices associated with the three assemblages begin to increase gradually, reaching a maximum at 6 m in the case of the bacterial assemblages, and reaching a maximum at 6.5 m in the case of archaeal and eukaryal assemblages. Intriguingly, the maximum predicted diversity metrics for each assemblage occurred as the halocline at DWR3 was traversed (Fig. 1), and with the exception of the eukaryal communities, remained comparatively high into the deep brine layer to a depth of 8 m (Fig. 4).

Individual phylogenetic reconstructions of the archaeal, bacterial, and eukaryal SSU rRNA genes sampled from the five water column depths yielded well-supported phylograms for use in examining the phylogenetic composition and structure of assemblages from these environments. We calculated Rao's index of phylogenetic diversity (D_P), a β-diversity metric that incorporates abundance weights for phylogenetic branch lengths associated with each assemblage, for each domain. D_P values associated with archaeal and eukaryal

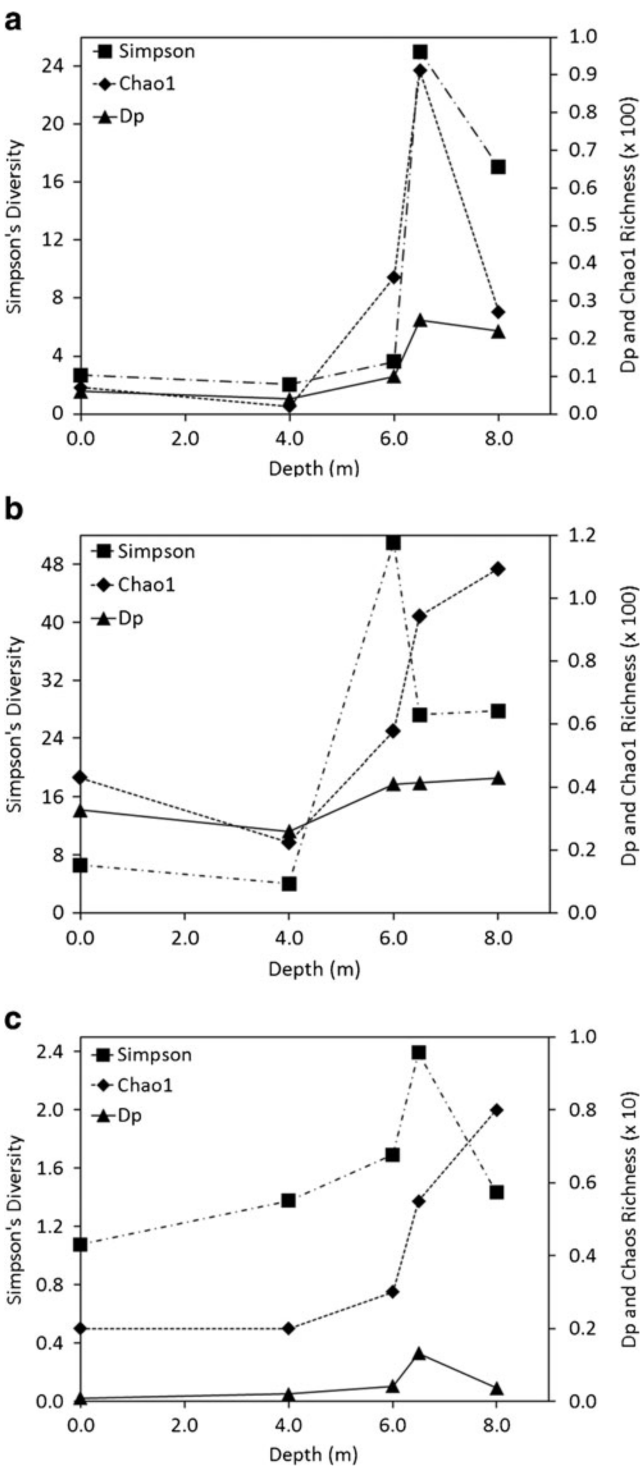

Fig. 4 Predicted Chao1 richness, Simpson's Index of diversity, and Rao's phylogenetic diversity (D_P) associated with archaeal 16S rRNA (**a**), bacterial 16S rRNA (**b**), and eukaryl 18S rRNA (**c**) gene assemblages as a function of water column depth

assemblages were greatest at a depth of 6.5 m, whereas only a small increase in the D_P associated with the bacterial community was observed as the halocline was traversed, reaching a maximum in the hypolimnion (Fig. 4). The D_P associated with archaeal assemblages exhibited a significant and inverse correlation with DO (Pearson R^2=0.84, p=0.03) whereas the D_P associated with eukaryal assemblages was most strongly correlated with PAR, although the relationship was not statistically significant (Pearson R^2=0.40, p=0.25) (data not shown). The D_P metric associated with bacterial assemblages was not strongly correlated with any measured variable.

Model selection and Mantel tests were used to quantify and rank the extent to which the phylogenetic relatedness of archaeal, bacterial, and eukaryal SSU rRNA gene assemblages reflected the characteristics of the environments from where they were sampled (Table 2). A dissimilarity matrix that describes the average Rao phylogenetic distance between lineages associated with one community when compared to lineages that comprise a second community served as the response variable. A model that describes all of the environmental parameters together (environmental matrix) was a strong predictor of the phylogenetic similarity of archaeal assemblages (Mantel R^2=0.74, p=0.02) but was a weak predictor of the similarity of bacterial and eukaryal assemblages (Mantel R^2=0.01 and 0.17, respectively; p=0.69 and 0.33, respectively) (Table 2). This observation suggests that bacterial and eukaryal lineages may be responding to individual environmental parameters that are masked when all parameters are considered together.

Of the individual parameters measured, the phylogenetic relatedness of archaeal SSU rRNA could best be predicted on the basis of the variation in temperature (ΔAICc=0.00, Mantel R^2=0.74, p=0.03); this relationship was statistically indistinguishable from a model that included salinity (ΔAICc=1.00, Mantel R^2=0.72, p=0.02) (Table 2). Given the covariance of temperature and salinity at DWR3, it is unclear which of these parameters, or both, is the true driver of community composition. The phylogenetic relatedness of bacterial communities could best be explained by variation in DO (ΔAICc=0.00, Mantel R^2=0.79, p=0.05) while the phylogenetic relatedness of the eukaryal assemblages could not be explained by any individual environmental parameters with statistical significance. The lack of a significant relationship between eukaryal communities and environmental parameters may be due to the presence of a dominant and nearly identical assemblage comprised of a single dominant alga (see below) in each of the 5 water column depths (Fig. 5), a feature that would lead to low phylogenetic signal and which would render community ecology approaches to characterizing shifts in community phylogenetic diversity less effective. The lack of correspondence observed here may also be due to the settling of algal biomass, as suggested by the dominance of algal taxa in assemblages below the halocline where PAR values are low.

Table 2 Model ranking using ΔAICc and Mantel correlation coefficients (R^2) where SSU rRNA Rao among community phylogenetic distance is the response variable. The p values were computed from 1000 Mantel regression permutations

Archaeal 16S rDNA				Bacterial 16S rDNA				Eukaryal 18S rDNA			
Model	ΔAICc	R^2	p	Model	ΔAICc	R^2	p	Model	ΔAICc	R^2	p
Temp	0.0	0.74	0.03	DO	0.0	0.79	0.05	Salinity	0.0	0.18	0.35
ENV[a]	0.2	0.74	0.02	Depth	13.1	0.22	0.07	DO	0.1	0.17	0.10
Salinity	1.0	0.72	0.02	PAR	15.0	0.05	0.36	ENV[a]	0.1	0.17	0.33
pH	9.3	0.35	0.07	pH	15.3	0.02	0.76	PAR	0.6	0.13	0.56
DO	10.2	0.29	0.12	Temp	15.5	0.01	0.76	Temp	1.1	0.08	0.47
Depth	13.0	0.05	0.48	ENV[a]	15.5	0.01	0.69	Depth	1.6	0.03	0.73
PAR	13.5	0.00	0.92	Salinity	15.5	0.00	0.80	pH	1.8	0.01	0.79

Abbreviations: *ΔAICc* difference in the Akaike Information Criterion for each model and the best model adjusted for small sample size; R^2 Mantel correlations coefficient; *p* p value derived from Mantel regression

[a] *ENV* an explanatory model that describes the variation in all five of the measured parameters (depth measurement excluded).

Taxonomic Composition of DWR3 Vertical Transect Microbial Communities

Both model selection and Mantel regression analyses indicate that the phylogenetic diversity of archaeal, bacterial, and eukaryal assemblages shift in response to environmental gradients, albeit to differing extents and in response to different factors. To identify specific lineages whose distribution is most influenced by environmental gradients, we examined the taxonomic composition of SSU rRNA gene assemblages as assessed by BLASTn analysis (Supp. Tables 2, 3 and 4; Fig. 5). In contrast to archaeal and eukaryal assemblages, which were dominated by a single taxonomic order (Supp. Tables 5 and 7), bacterial assemblages were more diverse (Supp. Table 6). Thus, order level assignments were chosen for this domain in attempt to simplify the analysis and identify the broader trends in the dataset.

Archaea

Archaeal 16S rRNA gene sequences generated from the transect along the DWR3 vertical profile revealed a unique species-level biodiversity that is generally not reflected from culture collections, as indicated by an average 94 % sequence identities (minimum=84 %, maximum=100 %) to cultivated representatives (Supp. Table 2and 5, Fig. 5a). The archaeal SSU rRNA gene communities sampled along the vertical transect were dominated by sequences affiliated with the archaeal order *Halobacteriales*. Several archaeal taxa dominated at each depth and exhibited clear trends with respect to physical and geochemical measurements (Supp. Table 8). The abundance of sequences affiliated with *Halogeometricum* sp. (range of 4.9 to 100.0 % of total sequences) were inversely correlated with salinity (Pearson R^2=0.95, p<0.01) and positively correlated with temperature (Pearson R^2=0.92, p<0.01) (Supp. Table 8). In contrast, the abundance of sequences affiliated with *Halonotius* sp. (range of 0.0 to 28.0 % of total sequences) was positively correlated with salinity (Pearson R^2=0.97, p< 0.01) and inversely correlated with temperature (Pearson R^2= 0.96, p<0.01). The abundances of sequences affiliated with *Haloquadratum* sp. (0.0 to 15.9 % of total sequences) and *Halosimplex* sp. (0.0 to 15.9 % of total sequences) both varied positively with salinity and inversely with temperature and DO. In addition to sequences affiliated with the *Halobacteriales*, sequences affiliated with the methanogens *Methanobrevibacter* sp. and *Methanohalophilus* sp. were identified. The abundance of both organisms were inversely correlated with DO and positively correlated with salinity.

Bacteria

Like the archaeal characterization, bacterial 16S rRNA gene sequences generated from each transect along the DWR3 vertical profile revealed a unique biodiversity that is generally absent from culture collections at the species level, as indicated by an average 94 % sequence identities (minimum=84 %, maximum=100 %) to cultivated representatives (Supp Table 3and 6, Fig. 5b). The abundance of several dominant bacterial orders varied with physicochemical measurements (Supp. Table 9). For example, the abundance of sequences affiliated with the bacterial orders *Chromatiales* (1.3 to 54.3 % of total) and *Rhodobacteriales* (5.0 to 20.0 % of total), (Supp. Table 5) were positively correlated with DO (Pearson R^2= 0.87 and 0.75, respectively; p values=0.07 and 0.17, respectively) (Supp. Table 9). In contrast, the abundance of sequences affiliated with the *Desulfobacterales* (0.0 to 17.6 % of total), and the Uncharacterized CFB (*Cytophaga–Flavobacteria–Bacteroides*) Group (0.0 to 18.9 % of total) were inversely correlated with DO (Pearson R^2=0.82 and 0.80, respectively; p=0.04 and 0.04, respectively). In addition to DO, the abundance of sequences affiliated with a number of bacterial orders exhibited strong correlations with other

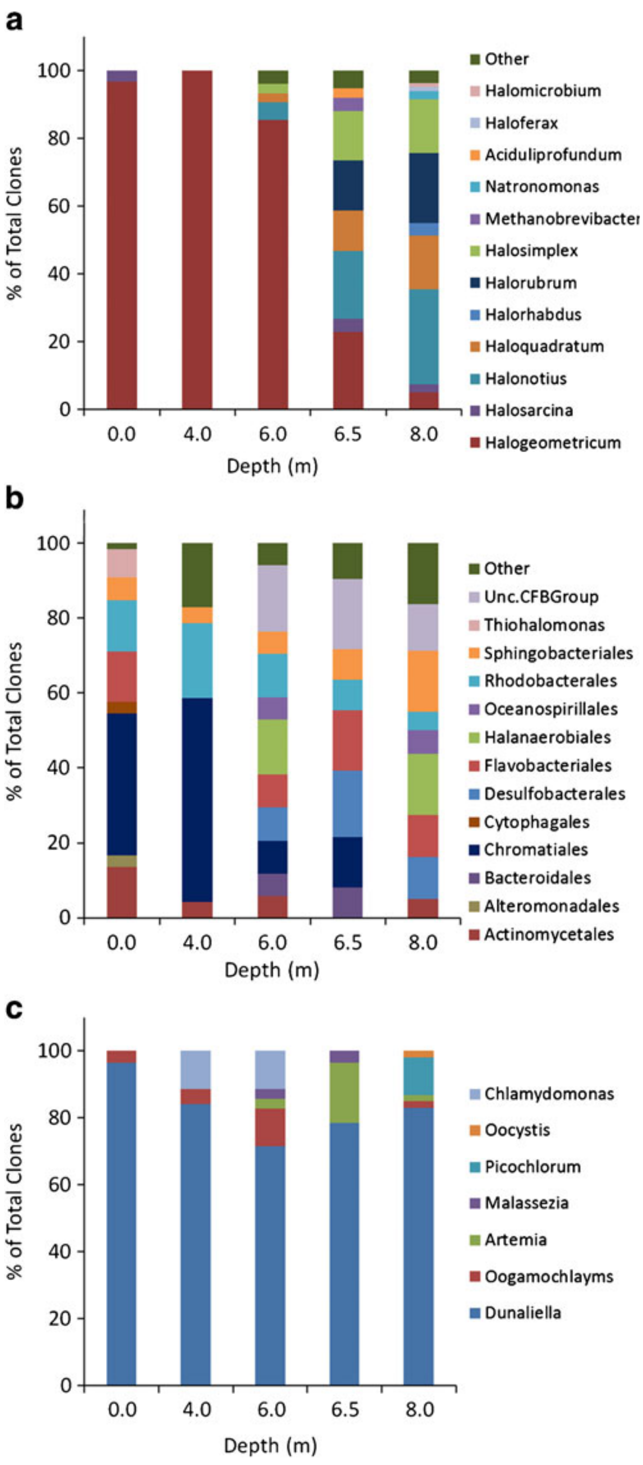

Fig. 5 Composition of archaeal (**a**), bacterial (**b**), and eukaryal (**c**) SSU rRNA gene assemblages from 0.0-, 4.0-, 6.0-, 6.5-, and 8.0-m depths, when binned at the genus, order, and genus level of taxonomy, respectively. Archaeal genera and bacterial orders that comprised <2 and <3 %, respectively, of each assemblage were combined and depicted as "other". Full taxonomic information for each assemblage is provided in Supplemental Tables 1, 2, 3, 4, 5, 6

physical and chemical measurements that are consistent with their inferred physiologies (Supp. Table 9).

Eukarya

The eukaryotic 18S rRNA gene libraries from the transect along the vertical profile of DWR3 were the least diverse of the domains examined, exhibiting an average percent identity to known taxa of 98 % (minimum=90 %, maximum=100 %) (Supp. Table 4 and 7, Fig. 5c). All of the eukaryal 18S rRNA gene assemblages sampled along the DWR3 vertical transect were dominated by algae affiliated with the taxonomic order *Chlamydomonadales* (range 78.6–100.0 % of total sequences). However, the composition of the algal component of the community shifted in response to environmental gradients. The abundance of sequences affiliated with the alga *Dunaliella* sp., the dominant alga in all transects of the water column (range 71.4 to 96.4 % of total sequences), was positively correlated with PAR (Pearson R^2=0.71; p=0.07) (Supp. Table 10). Likewise, sequences affiliated with the alga *Oogamochlamys* were primarily identified from the 0 to 6 m depths, the abundance of which varied positively with pH and inversely with salinity (Pearson R^2=0.47 and 0.33), albeit without strong statistical support. Sequences affiliated with *Chlamydomonas* sp. within the green algal class *Chlorophyceae* were identified at the 6.0 and 6.5 m depths, while sequences affiliated with *Picochlorum* within the algal class *Trebouxiophyceae* were only identified at the 8 m depth. In addition to algae, eukaryal assemblages from deeper depths (≥6 m) in the vertical transect contained sub-dominant sequences (<18 % of total sequences) affiliated with the arthropod *Artemia* sp. (1.1 to 17.9 % of total) and the fungus *Malassezia* sp. (0.0 to 3.6 % of total); the abundance of these genera did not vary significantly with any of the parameters measured in this study (Supp. Table 10).

Discussion

The strong gradients in physical and chemical parameters present in the DWR3 vertical transect of the GSL provide the unique opportunity to examine patterns in the mechanism of archaeal, bacterial, and eukaryal community assembly as a function of environment. Here, using phylogenetic approaches applied to a Sanger sequenced SSU rRNA gene dataset [5, 7], we assessed the relative importance of physiological or ecological constraints imposed by the environment (i.e., environmental filtering) and interspecies competition as controls on the phylogenetic structure and composition of individual archaeal, bacterial, and eukaryal assemblages inhabiting DWR3. Importantly, we also examined the structure of communities for evidence for stochastic or neutral -based processes [11] in the assembly of DWR3 assemblages. While evidence for a role for neutral-based processes was observed, in particular in the hypolimnion when null model 3 was employed in NRI calculations, the multiple lines of evidence, most importantly the strong capacity to predict the composition of archaeal and bacterial communities along the DWR3 gradient as a function of geochemistry, suggest that deterministic niche-based processes are likely the predominant influences on the assembly of communities along the DWR3 vertical transect. Nonetheless, the observation that p values for NRI were not all significant suggests an important, and likely secondary, role for stochastic processes in the assembly of DWR3 assemblages, in particular at or below the halocline.

A shift in the predominant mechanism of assembly from that of phylogenetically clustered communities to that of phylogenetically overdispersed assemblages along the DWR3 vertical transect was influenced by the characteristics of the environment. Here, the assembly of communities sampled from the epilimnion was found to be influenced primarily by environmental filters whereas the assembly of those sampled from the hypolimnion was influenced primarily by competitive interactions. The extent of phylogenetic overdispersion, as assessed by the net relatedness index (NRI), was positively correlated with salinity and inversely correlated with DO. It is not clear how salinity itself would directly lead to greater competitive interactions among populations comprising an assemblage. Rather, it is proposed that the strong association observed between the extent of phylogenetic overdispersion and salinity is due to the stratification of GSL due to differences in brine density which affects the rate of mixing between layers, imposes nutrient limitation in the hypolimnion, and creates strong gradients in other physical and chemical variables. In support of this model, a previous assessment of isopleths of water column temperature at a site in the south arm of GSL concluded that the differences in brine densities prevent significant mixing between the epilimnion and the hypolimnion, which creates gradients in nutrients such as phosphorus and nitrate [21]. In the present study, the concentration of DO in the south arm of GSL was also found to systematically decrease with depth, with the hypolimnion containing ~20 % of the DO concentration present in the surface waters. Nutrient limitation would be expected to limit the coexistence of species with overlapping fundamental niches that relate to O_2 toxicity or utilization [9], leading to phenotypic repulsion [1] and communities comprised of more distantly related species than would be expected based on the species richness of an assemblage and the patterns identified here [9].

The diversity of archaeal, bacterial, and eukaryal SSU rRNA gene assemblages, as assessed using both alpha and beta metrics, increased systematically with depth, reaching a maximum at the halocline (6–6.5 m depth). In other interfacial ecosystems such as riparian zones [39] and soils [40], the strength and periodicity of mixing between adjacent ecological systems across spatial and temporal scales creates physical, chemical, and biological heterogeneity that is the source of a multitude of habitats supporting vast biological and functional diversity [41]. Thus, the interface between the epilimnion and the hypolimnion and the physical and chemical heterogeneity that it creates at the DWR3 halocline may create additional ecological niches capable of supporting a greater diversity. Indeed, a recent study of mat communities in salterns in Guerrero Negro, Mexico which exhibit significant gradients and redox interfaces revealed significant shifts in community composition that were related to chemical gradients [42]. Likewise, a recent study found that the functional diversity of microbial communities inhabiting the interface between surface and deep brines in GSL is greater than that observed in the adjacent ecological systems [43]. Interestingly, this increase in functional diversity observed at the interface was not accompanied by an increased taxonomic phylogenetic diversity, an observation that the authors attribute to extensive horizontal gene transfer within the ecosystem [43].

The phylogenetic composition of archaeal, bacterial, and eukaryal communities inhabiting the DWR3 water column could be accurately predicted on the basis of environmental parameters, most notable salinity, DO, and temperature; both DO and temperature co-vary with salinity. These results are in agreement with previous reports which implicate salinity gradients as the primary driver of the phylogenetic similarity of bacterial assemblages [44] and bacterial/archaeal assemblages [45] in globally distributed microbiomes, including GSL. Since microorganisms inherit their ecological predilections from their ancestors [2, 10] with the exception of cases of horizontal gene transfer [46], this finding suggests that the populations that comprise the communities along the DWR3 gradient, characterized here by taxonomic genes, show conservatism in their habitat types. An examination of the inferred physiology of the dominant populations that comprise each assemblage in the DWR3 also supports this notion.

The abundance of 16S rRNA genes affiliated with the *Halogeometricum* decreased with increasing salinity whereas the abundance of sequences affiliated with several other genera (e.g., *Halorubrum*) increased with increasing salinity. Among the bacteria, the abundance of 16S rRNA genes affiliated with the *Chromatiales* decreased with increasing salinity and decreasing DO, whereas the abundance of *Desulfobacterales* and the uncharacterized CFB group increased systematically with increasing salinity and decreasing DO. The strain most closely affiliated with the *Chromatiales* identified in this study is *Aquisalimonas asiatica*, an aerobic halophile that prefers lower salinities [47], consistent with its distribution in the epilimnion. In contrast, the sequences that cluster with the *Desulfobacterales*, which were more prevalent in the low DO hypolimnion, are most closely related to a number of genera that are known to reduce sulfate [48] including *Desulfohalobium utahense* that was isolated from GSL[48]. Likewise, the predominant CFB sequence detected in the deeper depths of DWR3 is related to *Prolixibacter bellariivorans*, a facultative anaerobe that ferments sugars and in the process generates mixed acids and likely H_2, considering that the organism harbors a mixed acid fermentation pathway [49]. These inferences are consistent with previous reports of the detection of H_2S, H_2, and acetate in the hypolimnion of GSL, where anaerobic taxa such as those mentioned above are likely to thrive [21, 50–52]. The abundance of sequences affiliated with the alga *Dunaliella* spp., the dominant alga across all depths, were positively correlated with PAR (Pearson R^2=0.71; p=0.07) (Supp. Table 10). This is not a surprising result, as *Dunaliella* spp. have consistently been reported as the major contributor to photosynthetic primary productivity in GSL [53].

In conclusion, the results presented here provide compelling evidence that deterministic processes have played an important role in defining the composition of microbial assemblages along the DWR3 vertical transect, in particular in the epilimnion. The non-random distribution of lineages along the DWR3 vertical profile, coupled with evidence of increasing phylogenetic diversity with depth and a transition in the mechanism of community assembly at the halocline suggests strong conservatism in their habitat types. Conservatism in habitat type is facilitated by conservatism in physiological traits, which enable biodiversity to persist in a given environmental context. Thus, one would expect to observe significant shifts in the functional diversity and metabolic potentials (e.g., shift from primarily aerobic to anaerobic taxa at halocline) as one transcends the DWR3 vertical transect. Indeed, recent evidence suggests that the distribution of a biomarker gene for anoxic bacterial organic carbon fermentation [i.e., [FeFe]-hydrogenase structural gene *hydA*] responsible for the production of H_2 in many environments [54] are absent from the epilimnion, but are abundant in the hypolimnion (E.S. Boyd, unpublished data). Thus, the results of this paper further underscore the utility of phylogenetic tools in ecological research aimed at improving understanding into the mechanisms that both underlie and control the composition and structure of communities in natural environments [1–3].

Acknowledgments The authors express their sincere gratitude to John Luft and colleagues at the Utah Division of Wildlife Resources, Great Salt Lake Ecosystem Project, for boat access, sampling help, and GIS expertise. The authors of this work gratefully acknowledge the United States Air Force Office of Scientific Research under grant FA9550-05-1-0365 and FA9550-11-1-0211 (to JEM, JWP, MCP, and ESB) and R-8196-G1 to JRS. We would also like to acknowledge the technical assistance of Devin Karns and Alex Trujillo as well as Shannon Ulrich and Dave Vuono for their careful review of a previous version of this manuscript.

References

1. Webb CO, Ackerly DD, McPeek MA, Donoghue MJ (2002) Phylogenies and community ecology. Annu Rev Ecol Syst 33:475–505
2. Wiens JJ, Graham CH (2005) Niche conservatism: Integrating evolution, ecology, and conservation biology. Annu Rev Ecol Evol Syst 36:519–539
3. Westoby M (2006) Phylogenetic ecology at world scale, a new fusion between ecology and evolution. Ecology 87:S163–S165
4. Boyd ES, Hamilton TL, Spear JR, Lavin M, Peters JW (2010) [FeFe]-hydrogenase in Yellowstone National Park: evidence for dispersal limitation and phylogenetic niche conservatism. ISME J 4:1485–1495
5. Bryant JB, Lamanna C, Morlon H, Kerkhoff AJ, Enquist BJ, Green JL (2008) Microbes on mountainsides: Contrasting elevational patterns of bacterial and plant diversity. Proc Natl Acad Sci USA 105:11505–11511
6. Hamilton TL, Boyd ES, Peters JW (2011) Environmental constraints underpin the distribution and phylogenetic diversity of *nifH* in the Yellowstone geothermal complex. Microb Ecol 61:860–870
7. Horner-Devine MC, Bohannan BJM (2006) Phylogenetic clustering and overdispersion in bacterial communities. Ecology 87: S100–S108
8. Newton RJ, Jones SE, Helmus MR, McMahon KD (2007) Phylogenetic ecology of the freshwater *Actinobacteria* acI lineage. Appl Environ Microbiol 73:7169–7176
9. Maherali H, Klironomos JN (2007) Influence of phylogeny on fungal community assembly and ecosystem functioning. Science 1746–1748
10. Wiens JJ (2004) Speciation and ecology revisited: phylogenetic niche conservatism and the origin of species. Evolution 58:193–197
11. Hubbell SP (2001) The unified neutral theory of biodiversity and biogeography Princeton University Press. Princeton, New Jersey
12. Kembel SW (2009) Disentangling niche and neutral influences on community assembly: assessing the performance of community phylogenetic structure tests. Ecol Lett 12:949–960
13. Vamosi SM, Heard SB, Vamosi JC, Webb CO (2009) Emerging patterns in the comparative analysis of phylogenetic community structure. Mol Ecol 18:572–592
14. Armitage DW, Gallagher KL, Youngblut ND, Buckley DH, Zinder SH (2012) Millimeter-scale patterns of phylogenetic and trait diversity in a salt marsh microbial mat. Frontiers in Microbiology 3:293
15. Webb CO (2000) Exploring the phylogenetic structure of ecological communities: an example for rain forest trees. Am Nat 156:145–155
16. Hamilton TL, Vogl K, Bryant DA, Boyd ES, Peters JW (2012) Environmental constraints defining the distribution, composition, and evolution of chlorophototrophs in thermal features of Yellowstone National Park. Geobiol 10:236–249
17. Hassibe WR, Keck WG (1978) The Great Salt Lake. US Geological Survey. Reston, VA
18. Cannon JS, Cannon MA (2002) The Southern Pacific Railroad Trestle—past and present. In: Gwynn, JW (ed.) Great Salt Lake, an overview of change. Special Publication of the Utah Department of Natural Resources, Salt Lake City, Utah, pp 283–294
19. Baxter BK, Litchfield CD, Sowers K, Griffith JD, DasSarma PA, DasSarma S (2005) In: Gunde-Cimerron N, Oren A, Plemenita A (eds) Adaptation to life in high salt concentrations in Archaea, Bacteria and Eukarya. Springer, Netherlands
20. Naftz D., Angeroth C, Kenney T, Waddell B, Darnell N, Silva S, Perschon C, Whitehead J (2008) Anthropogenic influences on the input and biogeochemical cycling of nutrients and mercury in Great Salt Lake, Utah, USA. Appl Geochem 23:1731–1744
21. Stephens DW, Gillespie DM (1976) Phytoplankton production in the Great Salt Lake, Utah, and a laboratory study of algal response to enrichment. Limnol Ocean 21:74–87

22. Graham CH, Parra JL, Rahbek C, McGuire JA (2009) Phylogenetic structure in tropical hummingbird communities. Proc Natl Acad Sci USA 106:19673–19678
23. Weiss RF (1970) The solubility of nitrogen, oxygen and argon in water and seawater. Deep Sea Res Oceanogr Abstr 17:721–735
24. Lane DJ (1991) 16S/23S rRNA sequencing. In: Stackenbrandt E, Goodfellow M (eds.) Nucleic acid techniques in bacterial systematics. John Wiley and Sons, New York, NY, pp 115–175
25. Spear JR, Walker JJ, McCollom TM, Pace NR (2005) Hydrogen and bioenergetics in the Yellowstone geothermal ecosystem. Proc Natl Acad Sci USA 102:2555–2560
26. Thompson JD, Higgins DG, Gibson TJ (1994) CLUSTAL W: improving the sensitivity of progressive multiple sequence alignment through sequence weighting, position-specific gap penalties and weight matrix choice. Nucleic Acids Res 22:4673–4680
27. Ashelford KE, Chuzhanova NA, Fry JC, Jones AJ, Weightman AJ (2006) New screening software shows that most recent large 16S rRNA gene clone libraries contain chimeras. Appl Environ Microbiol 72:5734–5741
28. Ashelford KE, Chuzhanova NA, Fry JC, Jones AJ, Weightman AJ (2005) At least 1 in 20 16S rRNA sequence records currently held in public repositories is estimated to contain substantial anomalies. Appl Environ Microbiol 71:7724–7736
29. Schloss PD, Handelsman J (2005) Introducing DOTUR, a computer program for defining operational taxonomic units and estimating species richness. Appl Environ Microbiol 71:1501–1506
30. Jost L (2006) Entropy and diversity. Oikos 113:363–375
31. Anisimova M, Gascuel O (2006) Approximate likelihood-ratio test for branches: a fast, accurate, and powerful alternative. Syst Biol 55:539–552
32. Guindon S, Gascuel O (2003) A simple, fast, and accurate algorithm to estimate large phylogenies by maximum likelihood. Syst Biol 52:696–704
33. Posada D (2006) ModelTest Server: a web-based tool for the statistical selection of models of nucleotide substitution online. Nucleic Acids Res 34:W700–W703
34. Swofford DL (2001) Paup: Phylogenetic analysis using parsimony (and other methods). Sinauer, Sunderland, MA
35. Webb CO, Ackerly DD, Kembel SW (2008) Phylocom: software for the analysis of phylogenetic community structure and character evolution. Bioinformatics 24:2098–2100
36. Boyd ES, Skidmore M, Mitchell AC, Bakermans C, Peters JW (2010) Methanogenesis in subglacial sediments. Environ Microbiol Rep 2:685–692
37. Goslee SC, Urban DL (2007) The ecodist package for dissimilarity-based analysis of ecological data. J Stat Softw 22:1–19
38. Johnson JB, Omland KS (2004) Model selection in ecology and evolution. Trends Ecol Evol 19:101–108
39. Naiman RJ, Décamps H, Pollock M (1993) The role of riparian corridors in maintaining regional biodiversity. Ecol Appl 3:209–212
40. Totsche KU, Rennert T, Gerzabek MH, Kögel-Knabner I, Smalla K, Spiteller M, Vogel H (2010) Biogeochemical interfaces in soil: The interdisciplinary challenge for soil science. J Plant Nutr Soil Sci 173:88–99
41. Curtis TP, Sloan WT (2005) Exploring microbial diversity—a vast below. Science 309:1331–1333
42. Harris JK, Caporaso JG, Walker JJ, Spear JR, Gold NJ, Robertson CE, Hugenholtz P, Goodrich J, McDonald D, Knights D, Marshall P, Tufo H, Knight R, Pace NR (2013) Phylogenetic stratigraphy in the Guerrero Negro hypersaline microbial mat. ISME J 7:50–60
43. Parnell JJ, Rompato G, Latta LCIV, Pfrender ME, Van Nostrand JD, He Z, Zhou J, Andersen G, Champine P, Ganesan B, Weimer BC (2010) Functional biogeography as evidence of gene transfer in hypersaline microbial communities. PLoS One 5:e12919
44. Lozupone CA, Knight R (2007) Global patterns in bacterial diversity. Proc Natl Acad Sci USA 104:11436–11440
45. Caporaso JG, Lauber CL, Walters WA, Berg-Lyons D, Lozupone CA, Turnbaugh PJ, Fierer N, Knight R (2010) Global patterns of 16S rRNA diversity at a depth of millions of sequences per sample. Proc Natl Acad Sci USA 108:4516–4522
46. Gogarten JP, Townsend JP (2005) Horizontal gene transfer, genome innovation and evolution. Nat Rev Micro 3:679–687
47. Márquez MC, Carrasco IJ, Xue Y, Ma Y, Cowan DA, Jones BE, Grant WD, Ventosa A (2007) *Aquisalimonas asiatica* gen. nov., sp. nov., a moderately halophilic bacterium isolated from an alkaline, saline lake in Inner Mongolia, China. Int J Syst Evol Microbiol 57:1137–1142
48. Garrity GM, Brenner DJ, Krieg NR, Staley JT (eds.) (2005) Bergey's manual of systematic bacteriology, vol. 2: The proteobacteria, Part C: The Alpha-, Beta-, Delta- and Epsilonproteobacteria. Springer, New York, NY
49. Holmes DE, Nevin KP, Woodard TL, Peacock AD, Lovley DR (2007) *Prolixibacter bellariivorans* gen. nov., sp. nov., a sugar-fermenting, psychrotolerant anaerobe of the phylum Bacteroidetes, isolated from a marine-sediment fuel cell. Int J Syst Evol Microbiol 57:701–707
50. Lupton FS, Phelps TJ, Zeikus JG (1984) Methanogenesis, sulphate reduction and hydrogen metabolism in hypersaline anoxic sediments of the Great Salt Lake, Utah. In: Editor (ed.)^(eds.) Book Methanogenesis, sulphate reduction and hydrogen metabolism in hypersaline anoxic sediments of the Great Salt Lake, Utah., vol. Bureau of Mineral Resources, City, pp. 42–48
51. Phelps T, Zeikus JG (1980) Microbial ecology of anaerobic decomposition in Great Salt Lake. Abstract 14, pp 89, 80th Annual Meeting of the American Society for Microbiology, American Society for Microbiology, Washington, D.C.
52. Zeikus JG (1983) Metabolic communication between biodegradative populations in nature. In: Slater, JH, Whittenbury E, and Wimpenny JWT (eds.) Microbes in their natural environments, Society for General Microbiology, Symposium 34, Cambridge University Press, Cambridge, MA
53. Rushforth S, Felix E (1982) Biotic adjustments to changing salinities in the Great Salt Lake, Utah, USA. Microb Ecol 8:157–161
54. Boyd ES, Spear JR, Peters JW (2009) [FeFe]-hydrogenase genetic diversity provides insight into molecular adaptation in a saline microbial mat community. Appl Environ Microbiol 75:4620–4623